

Z=50 shell gap near ^{100}Sn from intermediate-energy Coulomb excitations in even-mass $^{106-112}\text{Sn}$ isotopes

C. Vaman¹, C. Andreoiu², D. Bazin¹, A. Becerril^{1,3}, B.A. Brown^{1,3}, C.M. Campbell^{1,3}, A. Chester^{1,3}, J.M. Cook^{1,3}, D.C. Dinca^{1,3}, A. Gade^{1,3}, D. Galaviz¹, T. Glasmacher^{1,3}, M. Hjorth-Jensen⁵, M. Horoi⁶, D. Miller^{1,3}, V. Moeller^{1,3}, W.F. Mueller¹, A. Schiller¹, K. Starosta^{1,3}, A. Stolz¹, J.R. Terry^{1,3}, A. Volya⁴, V. Zelevinsky^{1,3}, and H. Zwahlen^{1,3}

¹National Superconducting Cyclotron Laboratory, Michigan State University, East Lansing, Michigan 48824, USA

²Department of Physics, University of Guelph, Guelph, Ontario, Canada N1G 2W1

³Department of Physics and Astronomy, Michigan State University, East Lansing, Michigan 48824, USA

⁴Physics Department, Florida State University, Tallahassee, Florida 32306, USA

⁵Department of Physics and Center of Mathematics for Applications, University of Oslo, N-0316, Oslo, Norway

⁶Department of Physics, Central Michigan University, Mount Pleasant, Michigan 48859, USA

(Dated: May 24, 2018)

Rare isotope beams of neutron-deficient $^{106,108,110}\text{Sn}$ nuclei from the fragmentation of ^{124}Xe were employed in an intermediate-energy Coulomb excitation experiment yielding $B(E2, 0_1^+ \rightarrow 2_1^+)$ transition strengths. The results indicate that these $B(E2, 0_1^+ \rightarrow 2_1^+)$ values are much larger than predicted by current state-of-the-art shell model calculations. This discrepancy can be explained if protons from within the $Z = 50$ shell are contributing to the structure of low-energy excited states in this region. Such contributions imply a breaking of the doubly-magic ^{100}Sn core in the light Sn isotopes.

PACS numbers: 25.70.De, 23.20.-g

Numerous experimental and theoretical studies are currently focused on nuclear structure evolution far from the line of stability. In particular, the structure of neutron-deficient nuclei near the $N=Z$ line is impacted by protons and neutrons occupying the same shell model orbitals. This letter reports observations which indicate that large spatial overlaps of valence orbitals in neutron-deficient, even-mass, tin isotopes, break the stability of the $Z=50$ shell gap near doubly-magic ^{100}Sn .

^{100}Sn is the heaviest, doubly-magic, $N=Z$, particle-bound nucleus and therefore is of great interest for shell theory of heavy nuclei. However, it is very difficult to produce and experimentally study this nucleus. One way to approach ^{100}Sn is to examine the evolution of nuclear properties along the $Z = 50$ chain of tin isotopes, which is the longest shell-to-shell chain of semi-magic nuclei investigated in nuclear structure to date. The nearly constant energy of the first excited 2_1^+ state between $N=52$ and $N=80$ [1], is one of the well known features of Sn isotopes, and it seems to indicate that effective nuclear interactions between nucleons of the same flavor outside a doubly-magic core do not affect the near-spherical nuclear shape [2]. A probe of the stability of the $Z=50$ shell gap is provided by the electromagnetic transition rates between the 0_1^+ ground and the first excited 2_1^+ state, in even mass Sn isotopes. Even small admixtures of proton excitations across the $Z=50$ shell gap enhance significantly the electric quadrupole transition probability between the ground and the first excited states in contrast to the configurations with the closed $Z=50$ core and only neutrons in the valence space.

While experimental 2_1^+ state energies are well established, the reduced probability for the electric quadrupole transition from the ground state to the first excited state, $B(E2, 0_1^+ \rightarrow 2_1^+)$, has been sparsely known except for

stable Sn isotopes. For neutron-rich tin nuclei, the measurements of these $B(E2)$ values have only recently been achieved due to progress in radioactive beam techniques [3]. On the neutron-deficient side, the corresponding numbers are still unknown except for ^{108}Sn measured recently in an intermediate-energy Coulomb excitation at GSI [4]. The measurements on the neutron-deficient side of the $Z=50$ chain are hindered by the 6_1^+ isomeric state with a lifetime in the nanosecond range, while the expected lifetime for the 2_1^+ state is at least two orders of magnitude shorter. Therefore, for a measurement, the 2_1^+ state must be populated from the ground state. Consequently, Coulomb excitation is the method of choice if beams of unstable nuclei are available, while other reactions, in particular fusion-evaporation, cannot be applied. This letter reports on the results of an intermediate energy Coulomb excitation experiment and the measurements of the corresponding $B(E2, 0_1^+ \rightarrow 2_1^+)$ strength of neutron-deficient $^{106-110}\text{Sn}$ isotopes from the fragmentation of ^{124}Xe . In addition, a measurement for ^{112}Sn is reported as a check of consistency with existing experimental data.

Beams of rare isotopes are produced via projectile fragmentation at the National Superconducting Cyclotron Laboratory (NSCL) as documented in [5]. In the current experiment a stable beam of ^{124}Xe was accelerated by the Coupled Cyclotron Facility to 140 MeV/nucleon and fragmented on a 300 mg/cm^2 thick Be foil at the target position of the A1900 fragment separator [6]. A combination of slits and a 165 mg/cm^2 Al wedge degrader were used at the A1900 to enhance the purity of the fragment of interest in the resulting cocktail beam. The properties of the Sn beams in this experiment are listed in Table I.

Coulomb excitation of the above cocktail beams on a

TABLE I: Properties of the rare isotope Sn beams used in the current experiment.

Isotope	Energy [MeV/u]	Purity [%]	$\Delta p/p$ [%]	Rate [10^3 pps/pnA]
^{112}Sn	80	50	0.10	19
^{110}Sn	79	50	0.10	21
^{108}Sn	78	17	0.34	17
^{106}Sn	81	2	0.34	0.7

212 mg/cm² thick ^{197}Au target were studied using a combination of the Segmented Germanium Array (SeGA) [7] for gamma-ray detection and the high resolution S800 spectrograph for particle identification and reconstruction of the reaction kinematics [8]. For all four tin isotopes studied, a lithium-like and a beryllium-like charge state were delivered to the S800 focal plane and identified by their position on the Cathode Readout Drift Chamber (CRDC) detectors [9]. The mass and charge of the nuclei were extracted on an event-by-event basis from the time of flight and energy loss information.

The S800 CRDC detectors measure position and angle in dispersive and non-dispersive directions at the focal plane. This information can be used to reconstruct the trajectories of identified particles to the target position based on the knowledge of the magnetic field in the S800 [8]. The proper trajectory reconstruction provides information on the scattering angle at the target, and, therefore, on the impact parameter in the Coulomb excitation process [10]. This information is crucial to relate the Coulomb excitation cross section at the intermediate energies to the reduced E2 transition probability. For the projectile excitation this relation is given by [11]:

$$\sigma_{proj}(E2, I_i \rightarrow I_f) \propto B(E2, I_i \rightarrow I_f) Z_{tar}^2 / b_{min}^2, \quad (1)$$

where b_{min} is the minimum impact parameter considered for the cross section measurement. The minimum impact parameter is chosen to be large enough to minimize the impact of nuclear force interference.

The procedure outlined above for a $B(E2, 0_1^+ \rightarrow 2_1^+)$ measurement from an angle-integrated Coulomb cross section has been applied in a number of successful experiments at the NSCL [11, 12, 13]. In the current study, however, the absolute Coulomb excitation cross section measurement was hindered by angular acceptance effects related to properties of the heavy mass and large charge beams. Thus, below, the experimental information on the transition rates was extracted from a relative measurement to excitations of the ^{197}Au target.

Following Eq. 1 the ratio of the cross sections for the Sn projectile and Au target excitations in the current experiment is given by:

$$\frac{\sigma_{Sn}(E2, 0_1^+ \rightarrow 2_1^+)}{\sigma_{Au}(E2, 3/2_1^+ \rightarrow 7/2_1^+)} = \frac{B_{Sn}(E2, 0_1^+ \rightarrow 2_1^+)}{B_{Au}(E2, 3/2_1^+ \rightarrow 7/2_1^+)} \left(\frac{79}{50} \right)^2 \quad (2)$$

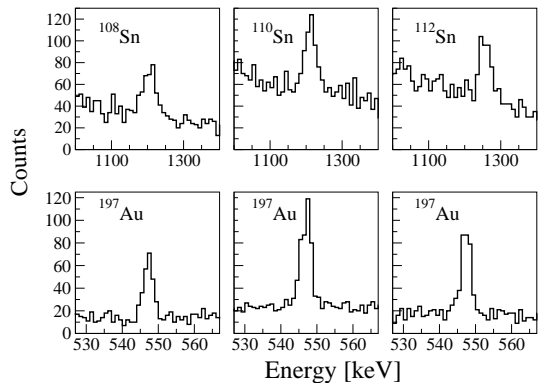


FIG. 1: Gamma-ray spectra measured by the 90° ring of the SeGA for the $^{108-112}\text{Sn}$ projectiles (top) and the corresponding Au target (bottom) Coulomb excitations within the 45 mrad scattering angle in the laboratory reference frame.

The dependence on b_{min} and the reaction kinematics in this ratio is removed as long as safe Coulomb conditions are met. The ratio of the cross sections is measured from the ratio of gamma-ray intensities depopulating the 2_1^+ state in Sn and the $7/2_1^+$ state in the Au nuclei. Knowing the target $B(E2 \uparrow)$ [14] the corresponding transition rate for the projectile is extracted.

In view of the above, the analysis of the $^{108-112}\text{Sn}$ data proceeded in the following way. A subset of particle-identified events with the impact parameter larger than 19.5 fm was selected; the corresponding scattering angle in the lab was 45 mrad. Next, the cross section ratio measurements were performed according to Eq. 2 for the downstream ring at 37° and the upstream ring at 90° separately, and the $B(E2 \uparrow)$'s in Sn nuclei were extracted from these ratios. Spectra illustrating the quality of the data for the 90° ring are shown in Fig. 1. The corresponding results are listed in Table II. It should be stressed that the precise value for the impact parameter is not crucial for this analysis.

TABLE II: Reduced E2 transition rates measured for $^{106-112}\text{Sn}$ isotopes. The results for $^{108-112}\text{Sn}$ correspond to the lab scattering angles smaller than 45 mrad, for the ^{106}Sn the scattering angle limit was set by the S800 spectrograph acceptance [8].

Isotope	$B(E2, 0_1^+ \rightarrow 2_1^+) [e^2 b^2]$	$\Delta_{stat} [e^2 b^2]$	$\Delta_{sys} [e^2 b^2]$
^{112}Sn	0.240	0.020	0.025
^{110}Sn	0.240	0.020	0.025
^{108}Sn	0.230	0.030	0.025
^{106}Sn	0.240	0.050	0.030

For the $B(E2, 0_1^+ \rightarrow 2_1^+)$ measurement in ^{106}Sn the off-line analysis requirement set on the impact parameter and the scattering angle was relaxed; however, the range of the scattering angles for detected events is still limited to 60 mrad by the angular acceptance of the S800 spectrograph. For all four isotopes the ratio of

the projectile to the target Coulomb excitations was extracted using the data shown in Fig. 2. A common scaling factor between these ratios and the measured $B(E2, 0_1^+ \rightarrow 2_1^+)$ values was computed for $^{108-112}\text{Sn}$ and applied to the ^{106}Sn ; the resulting $B(E2)$ for ^{106}Sn is reported in Table II.

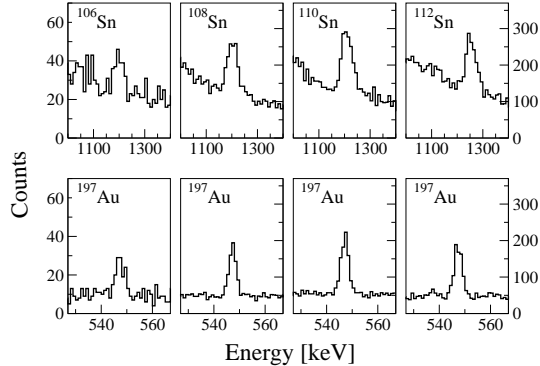


FIG. 2: Gamma-ray spectra measured with SeGA for the $^{106-112}\text{Sn}$ projectile (top) and the corresponding target (bottom) Coulomb excitations within the scattering angle limited by the S800 spectrograph acceptance.

Experimental information on the $B(E2, 0_1^+ \rightarrow 2_1^+)$ systematic in Sn isotopes based on the current measurement and Refs. [1, 3, 4] is presented in Fig. 3. The asymmetric behavior of the $B(E2 \uparrow)$ with respect to the $N=66$ neutron mid-shell at $A=116$ is striking. This is in disagreement with several shell model $B(E2 \uparrow)$ predictions including these from the Large Scale Shell Model calculations of Ref. [4] performed with a ^{90}Zr core, see Fig. 4 for the comparison. Shell model calculations consistently predict a $B(E2 \uparrow)$ trend which is nearly parabolic and symmetric with respect to the midshell [4, 15]. It reflects properties of the even-rank E2 tensor operator in the seniority scheme [2]. In regard to other recently proposed theories, the experimental $B(E2 \uparrow)$ strength is underpredicted by the Exact Pairing model of Ref. [15]. It should also be pointed out that while the predictions of Relativistic Quasiparticle Random Phase Approximation of Ref. [16] are consistent with the $B(E2 \uparrow)$ values measured here for the most neutron-deficient Sn isotopes, the overall trend for the Sn isotopic chain in the middle of the shell is not well reproduced by these calculations.

An effect which can explain large $B(E2 \uparrow)$ values in the neutron-deficient Sn isotopes may arise from correlation energy associated with nucleons occupying the same orbitals near $N=Z$ line. An analogy can be drawn between the Sn and Ni isotopic chains. The $^{56-78}\text{Ni}$ isotopes have valence neutron configurations, $(f_{5/2}, p_{3/2}, p_{1/2}, g_{9/2})^{A-56}$, similar in shell structure to those of $^{100-132}\text{Sn}$, $(g_{7/2}, d_{5/2}, d_{3/2}, s_{1/2}, h_{11/2})^{A-100}$. Effective charges take into account coupling between the valence nucleons and the proton particle-hole excitations of the core not included in the model space. The em-

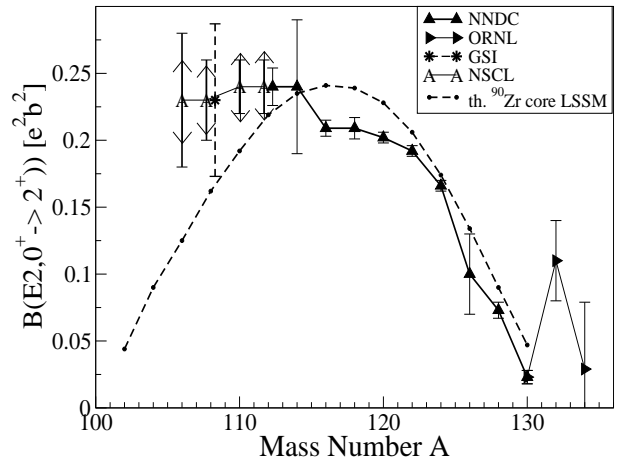


FIG. 3: Experimental data on $B(E2, 0_1^+ \rightarrow 2_1^+)$ in Sn isotopic chain from the current results for $^{106-112}\text{Sn}$ and from Refs. [1, 3, 4]. The dotted line shows the predictions of the Large Scale Shell Model calculations of Ref. [4] performed with ^{90}Zr core. For $^{106-112}\text{Sn}$ the error bars represent statistical errors; the corresponding systematic errors are marked by arrows.

pirical values of $e_p = 1.2$ and $e_n = 0.8$ [17] apply to the full pf shell, and thus take into account coupling to the $2\hbar\omega$ giant isoscalar and isovector quadrupole excitations [18]. The $B(E2 \uparrow)$ excitation strengths obtained in the $(f_{5/2}, p_{3/2}, p_{1/2})$ model with the GXPF1 interaction [19] are 0.0126, 0.0249, 0.0264, 0.0243 and 0.0203 $e^2 b^2$ for $^{58,60,62,64,66}\text{Ni}$ compared to experimental values [1] of 0.0695(20), 0.0933(15), 0.0890(25), 0.0760(80) and 0.0620(90) $e^2 b^2$, respectively. The full pf shell results (including the $f_{7/2}$ orbit) obtained with GXPF1 are $B(E2) = 0.065, 0.106, 0.119, 0.082$ and $0.047 e^2 b^2$, respectively[21]. The coupling of valence neutrons to the low-lying $1p1h$ proton excitations $[(f_{5/2}, p_{3/2}, p_{1/2})(f_{7/2})^{-1}]$ of the Ni core could be taken into account by increasing the neutron effective charge from 0.8 to about 1.1 for all of the Ni isotopes leading to $B(E2) = 0.024, 0.047, 0.050, 0.046$ and $0.038 e^2 b^2$. Thus, in analogy, the effective charge of $e_n = 1$ used for $^{112-130}\text{Sn}$ in Ref. [4] for calculations with the ^{100}Sn core takes into account both the low-lying and high-lying ($2\hbar\omega$) quadrupole vibrations.

But effective charge is not enough to account for the large increase in the $B(E2 \uparrow)$ value for light Ni isotopes in the full pf model space compared to that obtained in the $f_{5/2}, p_{3/2}, p_{1/2}$ model space. To better understand the full pf model-space result for ^{58}Ni we need to consider the type of two-proton excitations leading to the $4p2h$ configuration shown schematically in Fig. 4 for ^{102}Sn . The low-lying spectrum of ^{58}Ni can be described by mixing of $2p$ and $4p2h$ configurations (relative to ^{56}Ni) with a collective band corresponding to the predominantly $4p2h$ state starting at 3.5 MeV [19]. This mixing leads to an enhanced $B(E2)$ for the ground state. The excitation energies of the multi-hole states [23] and the $B(E2)$ values [22] slowly converge to their full-space

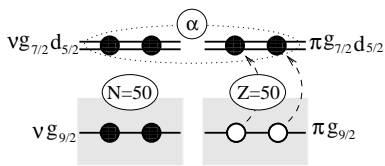


FIG. 4: Schematic representation of proton $2p2h$ excitations across the $Z=50$ shell gap in ^{102}Sn . The occupation of the same proton and neutron orbitals above the $Z=N=50$ shell leads to α -like correlations between the valence nucleons.

values as a function of the number of nucleons excited from the $f_{7/2}$ orbital. The $4p2h$ state is low in energy due to the alpha-correlation energy in the $4p$ structure as well as the pairing energy in the $2h$ structure. The alpha-correlation energy is particularly large near $N = Z$ when protons and neutrons are in the same orbital, and when the valence configuration is “open” in the sense that many two-particle couplings are allowed. As neutrons are added to ^{56}Ni , the alpha-correlation energy drops as the $f_{5/2}, p_{3/2}, p_{1/2}$ neutron orbitals become filled (and hence less “open”). To complete the analogy with Sn, improved results in comparison to experiment for the middle of the Ni isotopes require the addition of the $g_{9/2}$ orbit [24].

Thus, by considering these results for the Ni isotopes we can qualitatively understand (1) the origin of the large neutron effective charge and (2) a proposed origin for further $B(E2 \uparrow)$ enhancement towards ^{100}Sn due to $2p2h$ proton excitations. In analogy to the pf calculations, we expect the full sdg model space results to converge slowly [22] as a function of the number of nucleons excited out of the $g_{9/2}$ orbit making the exact calculation difficult.

The $2p2h$ excitations across the $Z=50$ shell gap and

α -like correlations discussed above also influence observables other than $B(E2 \uparrow)$'s. The correlations are likely to impact the α -decay rates for nuclei above ^{100}Sn . Next, low-lying 0^+ states in the light Sn isotopes built predominantly on $2p2h$ proton excitations are expected to exist close to the ground state with collective bands built on top of them. Last, a smooth band termination [25] is expected for these bands due to the limited valence space. All these can be addressed experimentally.

In summary, the measured nearly constant $B(E2, 0_1^+ \rightarrow 2_1^+)$ strength of $\sim 0.24 e^2 b^2$ in $^{106-110}\text{Sn}$ isotopes is in disagreement with the current state-of-the-art shell model predictions. This discrepancy could be explained if protons from within the $Z = 50$ shell contribute to the structure of low-energy excited states in this region. Such contributions are favored and stabilized by the α -like correlations for protons and neutrons occupying the same shell model orbitals. This result indicates breaking of the $Z = 50$ and $N=50$ gaps near the doubly-magic ^{100}Sn .

Acknowledgments

This work is supported by the US National Science Foundation Grants No. PHY01-10253, PHY-0555366 and NSF-MRI PHY-0619407. One author (C.A.) would like to acknowledge the support received from the National Science and Engineering Research Council of Canada, the Swedish Foundation for Higher Education and Research and the Swedish Research Council. The authors would like to acknowledge computational resources provided by the MSU High Performance Computing Center and Center of High Performance Scientific Computing, at Central Michigan University.

-
- [1] S. Raman, C.W. Nestor Jr and P. Tikannen, *At. Data Nucl. Data Tables* **78** (2001) 1.
 - [2] R. Casten, *Nuclear Structure from a Simple Perspective*, Oxford University Press, 2001.
 - [3] D.C. Radford *et. al*, *Nucl. Phys.* **A752** (2005) 264c.
 - [4] A. Banuet. *al*, *Phys. Rev.* **C72**, (2005) 061305(R).
 - [5] A. Stolz *et. al*, *Nucl. Instr. & Methods* **B241** (2005) 858.
 - [6] D.J.Morrissey *et. al*, *Nucl. Instr.& Meth.***B204**(2003) 90.
 - [7] W.F.Mueller *et. al*, *Nucl. Instr. & Meth.* **A466** (2001) 492.
 - [8] D. Bazin *et. al*, *Nucl. Instr. & Meth. Phys. Res.* **B204** (2003) 629.
 - [9] J. Yurkon *et. al*, *Nucl. Instr. & Meth.***A422** (1999) 291.
 - [10] A. Winther and K. Alder, *Nucl. Phys.* **A319** (1979) 518.
 - [11] T. Glasmacher, *Ann. Rev. Nucl. Part. Sci.* **48** (1998) 1.
 - [12] J. M. Cook, T. Glasmacher, A. Gade, *Phys. Rev.* **C73**, (2006) 024315.
 - [13] A. Gade *et. al*, *Phys. Rev.* **C68**, (2003) 014302.
 - [14] C. Zhou, *Nucl. Data Sheets* **76**, 399 (1995).
 - [15] A. Volya and V. Zelevinsky, *Nucl. Phys.* **A752** (2005) 325.
 - [16] A. Ansari, *Phys. Lett.* **B623** (2005)37.
 - [17] D. C. Dinca, *et al.*, *Phys. Rev.* **C71**, (2005) 041302(R).
 - [18] B. A. Brown, A. Arima and J. B. McGrory, *Nucl. Phys.* **A277**, (1977) 77 .
 - [19] M. Honma, T. Otsuka, B. A. Brown and T. Mizusaki, *Phys. Rev.* **C65**, (2002) 061301(R); *Phys. Rev.* **C69**, (2004) 034335.
 - [20] The three $f_{5/2}, p_{3/2}, p_{1/2}$ single-particle energies are readjusted to reproduce the spectrum of ^{57}Ni . For the $B(E2)$ We use harmonic-oscillator radial wavefunctions with $b = 1.01 A^{1/6}$.
 - [21] K. L. Yurkewicz, *et al.*, *Phys. Rev.* **C70**, (2004) 054319.
 - [22] F. Nowacki, *Nucl. Phys.* **A704**, (2002) 223c.
 - [23] M. Horoi, B. A. Brown, T. Otsuka, M. Honma, T. Mizusaki, *Phys. Rev.* **C73**, (2006) 061305(R).
 - [24] A. F. Lisetskiy, B. A. Brown, M. Horoi and H. Grawe, *Phys. Rev.* **C70**, (2004) 044314.
 - [25] A.V. Afanasjev, D.B. Fossan, G.J. Lane and I. Ragnarsson, *Phys. Rep.* **322** (1999) 1.